Received December 14, 2017, accepted January 23, 2018, date of publication February 9, 2018, date of current version March 13, 2018.
Digital Object Identifier 10.1109/ACCESS.2018.2804486

Nested Array Sensor With Grating Lobe Suppression and Arbitrary Transmit–Receive Beampattern Synthesis

ZHE WANG, WEN-QIN WANG, (Senior Member, IEEE), ZHI ZHENG, AND HUAIZONG SHAO
School of Information and Communication Engineering, University of Electronic Science and Technology of China, Chengdu 611731, China
Corresponding author: Wen-Qin Wang (wqwang@uestc.edu.cn)

ABSTRACT Sparse arrays have potential advantages over their regularly spaced counterparts, but they will generate undesired grating lobes. This paper investigates a sparse linear phased-array for grating lobe suppression and arbitrary transmit–receive beampattern synthesis. To achieve these aims, a modified two-level nested-array is developed, which provides increased degrees-of-freedom than a standard uniform linear array with the same number of elements via the difference co-array processing algorithm in the receiver. A least squares and iterative algorithm is also devised for linear array arbitrary transmit–receive beampattern design with minimum number of antenna elements. Moreover, the nested-array design is exploited for minimum variance distortionless response adaptive beamforming and direction finding. The effectiveness of the proposed approach is verified through extensive numerical results.

INDEX TERMS Sparse array, grating lobe, linear array, difference co-array, polynomial factorization, least squares, array synthesis.

I. INTRODUCTION

Phased arrays have been successfully applied in communication, radar and navigation systems [1]. Conventional uniform phased-arrays are expensive and heavy to yield wide aperture because a large number of radiating elements with interspacing of $\lambda/2$, where λ is the wavelength, are required to avoid grating lobes. On the other hand, nonuniform and/or sparse array deployments are also widely employed [2]–[8], because they have potential advantages over the standard regularly-spaced setting. In the literature, there are two main objectives of sparse array design, namely, array resolution enhancement which is often achieved through minimizing the peak sidelobe level and mainlobe width, and elimination of interferences via beamforming. Solutions based on genetic algorithm [9]–[11], random spacing [12], analytical sequences [13], [14], linear programming [15], and hybrid approach [16] have been proposed for phased-array thinning. In particular, multiple algorithmic strategies are developed in [17] for sparse periodic array design by combining transmit and receive aperture functions. However, only radiation patterns corresponding to unity-coefficient polynomials can be handled and extension to arbitrary arrays is not addressed. Additionally, compressive sensing-based array design is an advanced solution [18], but it is difficult for a large scale arbitrary beampattern synthesis and grating lobe suppression is often not considered.

More importantly, sparsening array elements have the potential drawbacks of generating grating lobes and reducing the control of the beam shape [19], but few techniques have been suggested so far for optimal deployment of sparse array elements and suppression of undesired grating lobes [20]–[23]. Placing array elements at periodic intervals exceeding $\lambda/2$ will create grating lobes and limit the usefulness of the array. It is because the quantized nature of the phase along the inputs of each element will degrade the array gain and pattern. Aperiodic placement can remove grating lobes and minimize sidelobe level. Although the relationship between the unit circle representation and antenna positions for aperiodic arrays has been derived in [24], array design remains a difficulty. Consequently, iterative search algorithms are often used to determine the required aperiodic antenna positions.

In this paper, the optimal sparse antenna array arrangement for grating lobe suppression with less elements is addressed. Given a fixed number of elements, the minimum redundancy array [25] is theoretically the optimum linear geometry which provides the maximum possible number of virtual elements. However, there is no closed-form expression for the structure of this array and hence the array geometry is not analytically tractable. Moreover, optimum design of a desired transmit-receive array beampattern is not easy, and in most cases, especially for a large array, we have to resort to complex computer simulations for the element placement [26]. Although array beampattern synthesis has received much attention, joint transmit-receive array beampattern synthesis has received relative little recognition. A polynomial factorization-based design of sparse periodic linear arrays has been proposed in [27], where the transmit and receive aperture polynomials are determined such that their product results in a polynomial representing the desired transmit-receive effective aperture function. Nevertheless, multiple possible combinations of transmit and receive arrays generally exist, while the optimum decomposition particularly for a large-scale array or high-order polynomial and grating lobe suppression are not investigated. Moreover, as in [17] and [27] focuses on the unity-coefficient polynomials. Recently, an interesting linear nested-array based on the concept of difference co-array [28] has been designed in [29]–[31] and extended to planar nested-array [32] and nested-array receiver with time-delayers for joint target range and angle estimation [33], which uses frequency diverse array (FDA), instead of phased-array. However, no study on grating lobe suppression and arbitrary array beampattern synthesis are discussed in the literature.

Inspired by the nested-arrays, the locations and weights of the elements for an arbitrary transmit-receive effective aperture function can be determined, such that a minimum number of antennas are involved and grating lobes are suppressed. It is also shown that the proposed method attains the total degrees-of-freedom (DOFs) of $N^2/2+1$ or $(N^2-1)/2+1$ where N denotes the number of available physical elements. Note that it is a phased-array, not multiple-input multiple-output (MIMO) radar. In the latter, the virtual array is equivalent to the Kronecker product of the transmit and receive array manifolds [34]. However, in the modified nested-array, the virtual array is formed through the difference co-array processing algorithm [28], [29]. Although active transmit beampattern is involved in the transmit-receive beampattern synthesis, the active transmit array is not employed in the difference co-array processing scheme.

In this paper, we have two objectives: (1) design arbitrary transmit-receive beampattern for a large-scale array, and (2) reduce the required number of array elements but without grating lobes. We proposed a modified two-level nested-array and choose the first-level as the transmitter such that the nulls of the transmit beampattern will coincide with the peaks of the receive beampattern to keep larger DOFs and utilize peak/null cancellation simultaneously so that the grating lobes can be suppressed. Although the idea of jointly designing two sparse vectors has been exploited in several papers [35]–[38], the motivation and solving method of this paper are thus different from the literature. The contributions of this work are summarized as follows: (i) The locations and weights of the transmit and receive elements are optimally computed, so that grating lobes are suppressed in the receiver; (ii) A modified nested-array is proposed, which provides more DOFs for a given number of physical elements N and without grating lobes; (iii) An arbitrary linear array transmit-receive beampattern of a large-scale array can be synthesized with the use of least squares (LS) and iterative algorithm, which excels the conventional polynomial factorization method, especially in designing a large-scale array with hundreds or even thousands of elements.

The remaining sections are organized as follows. Section II presents the arrangement of transmit and receive elements, which allows for suppressing the grating lobes. Section III is dedicated to the modified two-level nested-array design for more DOFs and suppressing grating lobes. Furthermore, an LS algorithm is proposed for arbitrary linear array beampattern synthesis. Receiver beamforming and direction finding based on the difference co-array are addressed in Section IV. Extensive simulations are included in Section V to verify the performance of the proposals. Finally, conclusions are drawn in Section VI.

II. ARRAY ARRANGEMENT WITH GRATING LOBE SUPPRESSION

It is well known that the array beampattern of an M-element uniform linear array (ULA) at the steering direction θ can be expressed as [27]

$$p_v(\theta)=\sum_{m=0}^{M-1} c_v[m]e^{j(2\pi(\sin(\theta)/\lambda)d)m}=p_v(x)=p_t(x)\cdot p_r(x) \tag{1}$$

where $c_v[m]$ is the element weighting function for the mth element, and d is the inter-element spacing. Let $x=e^{j2\pi(\sin(\theta)/\lambda)d}$, the decomposition factors $p_t(x)$ and $p_r(x)$ are expressed, respectively, as

$$p_t(x)=\sum_{i=0}^{T_e-1} c_t[i]x^i \tag{2a}$$

$$p_r(x)=\sum_{j=0}^{R_e-1} c_r[j]x^j \tag{2b}$$

where T_e and R_e are the numbers of elements including the missing elements in the transmit and receive arrays, and $c_t[i]$ and $c_r[j]$ denote respectively the element weights in the transmit and receive arrays. In [39], it is demonstrated that the combination of an N_t-element excluding the missing elements ULA spaced by $N_r\lambda/2$ in transmit array and an N_r-element (excluding the missing elements) ULA spaced by $\lambda/2$ in the receive array is equivalent to a ULA consisting of N_tN_r elements spaced by $\lambda/2$, where one antenna transmits a waveform and N_tN_r antennas receive the returns. This observation is further extended to the following corollary:

Corollary: The grating lobes can be suppressed when the N_t elements are spaced by $d_t=N_rd_r$ in the transmit (receive) array and N_r elements are spaced by $d_r=\lambda/2$ in the receive

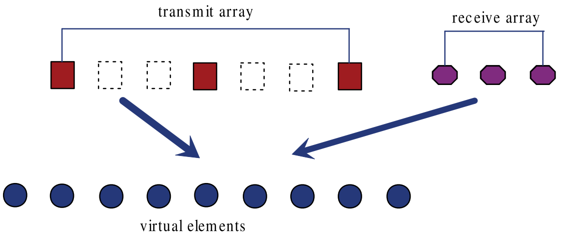

FIGURE 1. Illustration of transmit and receive array arrangement and their equivalent virtual elements.

(transmit) array. An illustration for $N_t = N_r = 3$ is provided in Fig. 1.

Proof: The array factors of the N_t-element ULA spaced by $N_r d_r$ and N_r-element ULA spaced by $d_r = \lambda/2$, denoted by $F_t(\theta)$ and $F_r(\theta)$, respectively, are given by

$$F_t(\theta) = \left| \frac{1}{N_t} \frac{\sin\left(\frac{N_t \pi}{\lambda} N_r d_r \sin\theta\right)}{\sin\left(\frac{\pi}{\lambda} N_r d_r \sin\theta\right)} \right| \quad (3)$$

$$F_r(\theta) = \left| \frac{1}{N_r} \frac{\sin\left(\frac{N_r \pi}{\lambda} d_r \sin\theta\right)}{\sin\left(\frac{\pi}{\lambda} d_r \sin\theta\right)} \right|. \quad (4)$$

The peaks of $F_t(\theta)$ will appear at [40]

$$\sin(\theta) = \frac{k\lambda}{N_r d_r}, \quad k = \pm 0, \pm 1, \ldots \quad (5)$$

Substituting (5) into (4) yields

$$F_r(\theta) = \left| \frac{1}{N_r} \frac{\sin(k\pi)}{\sin\left(\frac{k\pi}{N_r}\right)} \right| = 0, \quad k = \pm 1, \pm 2, \ldots \quad (6)$$

At the angles specified by (5), we obtain

$$F_t(\theta) F_r(\theta) = 0, \quad k = \pm 1, \pm 2, \ldots \quad (7)$$

Therefore, the grating lobes are suppressed in this case. ■

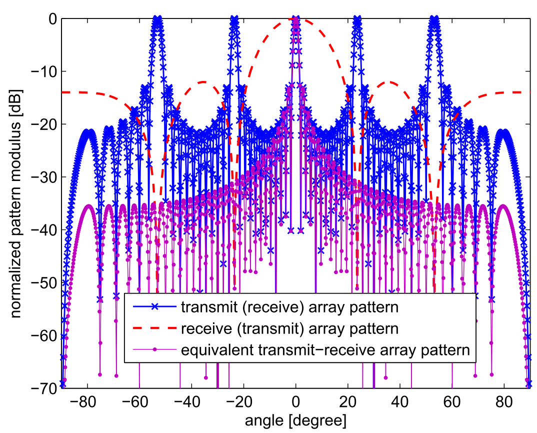

FIGURE 2. Comparative transmit, receive and equivalent array patterns.

As an example, Fig. 2 shows the comparative transmit, receive and effective transmit-receive patterns with $N_t = 12$, $N_r = 5$, $d_r = \lambda/2$, $\theta = 0°$ and $d_t = 5\, d_r$. It is apparent that the transmit (receive) grating lobes are suppressed by the nulls generated by the receive (transmit) array. This grating suppression characteristic is referred to as null-grating-lobe suppression [39].

Mathematically, the problem of the sparse array design with minimum number of elements and grating lobe suppression can then be formulated as

$$\begin{aligned} &\min \{N_t + N_r\} \\ &\text{s.t. } p_t(x) \cdot p_r(x) = p_v(x) \\ &\quad d_t = N_r d_r \text{ or } d_r = N_t d_t. \end{aligned} \quad (8)$$

Unless stated otherwise, the transmit and receive arrays can be swapped in the following discussion. It is required to use the minimum number of elements to achieve the desired effective transmit-receive pattern.

The problem of (8) can also be interpreted as decomposing $p_v(x)$ into $p_t(x)$ and $p_r(x)$ in an optimal sense. Once the optimum decomposition is determined, it is possible to transform the polynomials back to the arrays to obtain the desired structures. Recently, extension of the decomposition for a general integer M has been studied in [27]. Nevertheless, this decomposition approach can only be applied when $p_v(x)$ is a unity-coefficient polynomial.

Moreover, if a large array design is needed which corresponds to a high-order polynomial, it is difficult to find the suitable $p_t(x)$ and $p_r(x)$ because there are numerous combinations that can produce the same $p_v(x)$. To overcome these disadvantages, the novel idea is to consider the decomposition of $p_v(x)$ as a general deconvolution problem, which can be solved by the LS algorithm.

According to (1), the coefficients of $p_v(x)$, $p_t(x)$ and $p_r(x)$ have the following convolution relation

$$\mathbf{c}_v = \mathbf{c}_t \circledast \mathbf{c}_r \quad (9)$$

with

$$\mathbf{c}_v = \begin{bmatrix} c_v[0] & c_v[1] & \ldots & c_v[M-1] \end{bmatrix}^T \quad (10a)$$

$$\mathbf{c}_t = \begin{bmatrix} c_t[0] & c_t[1] & \ldots & c_t[T_e-1] \end{bmatrix}^T \quad (10b)$$

$$\mathbf{c}_r = \begin{bmatrix} c_r[0] & c_r[1] & \ldots & c_r[R_e-1] \end{bmatrix}^T \quad (10c)$$

where $\circledast$ and ^{T} denote the convolution and transpose operators, respectively.

Define $\mathbf{A}_t \in \mathbb{C}^{(R_e+T_e-1)\times T_e}$ and $\mathbf{A}_r \in \mathbb{C}^{(T_e+R_e-1)\times R_e}$:

$$\mathbf{A}_t = \begin{bmatrix} \mathbf{c}_r & & & \\ & \mathbf{c}_r & & \\ & & \ddots & \\ & & & \mathbf{c}_r \end{bmatrix} \quad (11a)$$

$$\mathbf{A}_r = \begin{bmatrix} \mathbf{c}_t & & & \\ & \mathbf{c}_t & & \\ & & \ddots & \\ & & & \mathbf{c}_t \end{bmatrix} \quad (11b)$$

Equation (9) can then be written as

$$\mathbf{c}_v = \mathbf{A}_t\mathbf{c}_t = \mathbf{A}_r\mathbf{c}_r. \tag{12}$$

Since $\mathbf{c}_v$ is a known vector, once N_t and N_r are determined, $\mathbf{c}_t$ and $\mathbf{c}_r$ can be obtained by LS. In this case, the optimization problem of (8) is reformulated as

$$\begin{aligned} &\min \{N_t + N_r\} \\ &\text{s.t. } \mathbf{c}_v = \mathbf{A}_t\mathbf{c}_t = \mathbf{A}_r\mathbf{c}_r \\ &\qquad d_t = N_r d_r \text{ or } d_r = N_t d_r. \end{aligned} \tag{13}$$

Prior to providing the solver for (13), this paper proposes a modified two-level nested-array in the next section, which can provide more DOFs to resolve sources.

III. MODIFIED TWO-LEVEL NESTED-ARRAY WITH INCREASED DOFS

It is well known that the number of sources that can be resolved with an N-element ULA using conventional subspace-based methods is $N-1$. To achieve higher DOFs, a receiver processing algorithm based on the concepts of difference co-array [28] and nested-array [29] is devised. To facilitate the development, the difference co-array and traditional two-level nested-array are first briefly reviewed as follows.

Definition 1 (Difference Co-Array): Consider an array with N elements and define the set

$$D = \left\{\mathbf{x}_i - \mathbf{x}_j\right\}, \quad \forall i, j = 1, 2, \ldots, N \tag{14}$$

where $\mathbf{x}_i$ is the position vector of the i-th element. The difference co-array is defined as the array whose elements are located at positions corresponding to the set D_e which consists of all the distinct elements in D.

The cardinality of D_e gives the DOFs that can be obtained from the difference co-array. Then the maximum attainable number of DOFs from a difference co-array with N elements, denoted by $\mathrm{DOF}_{\max}$, is:

$$\mathrm{DOF}_{\max} = N(N-1) + 1. \tag{15}$$

However, if a difference occurs more than once, it implies a decrease in the overall cardinality of D_e. Consider a linear array with d as the minimum spacing of the underlying grid and define the function $c[m]$ which takes a value 1 if there is an element located at md and 0 otherwise. The number of same occurrences in each position, denoted by γ, is expressed as

$$\gamma = c[m] \circledast c[-m]. \tag{16}$$

That is to say, the difference co-array of an N-element ULA is another ULA with $(2N-1)$ elements. It just indicates the fact that the maximum number of DOFs is always strictly less than $N(N-1)+1$. The attainable DOFs can be computed by the two-level nested-array method [29].

Definition 2 (Two-Level Nested-Array): It is basically a concatenation of two ULAs, namely, inner and outer ULAs where they consist of N_t and N_r elements with spacings d_t and $d_r = (N_t + 1)d_t$, respectively.

It is easily understood that the difference co-array of the two-level nested-array is a full ULA with $2N_r(N_t+1)-1$ elements whose positions are

$$\{md_t, m = -M, -M+1, \ldots, M, M = N_r(N_t+1) - 1\}. \tag{17}$$

This is a systematic way to increase the DOFs and the details can be found in [29].

Now, we are going to solve (13) by deploying the elements in the two levels such that the element number is minimized and the grating lobes are suppressed. Different from the conventional two-level nested-array [29] where all elements are acted as receiver only, the proposal uses the first-level array as both transmitter and receiver while keeping the second-level array as receiver only. For this setup, there will be grating lobes in the second-level array if the elements are deployed as in [29]. With the use of Corollary 1, the following modified two-level nested-array can then be designed for grating lobe suppression.

Definition 3 (Modified Two-Level Nested-Array): The proposed two-level nested-array is also a concatenation of two ULAs, namely, inner and outer arrays where the former has N_t elements with spacing d_t and the latter has N_r elements with spacing d_r such that $d_r = N_t d_t$. In doing so, the null-grating-lobe suppression scheme of Corollary 1 can be applied.

Similar to the basic nested-array, the virtual array is formed only by the passive receive phased-array through the difference co-array processing algorithm, which forms a virtual linear array with the element spacing of $\lambda/2$. In doing so, the grating lobes will be suppressed. Therefore, the difference co-array of the modified two-level nested-array is a full ULA with $2N_tN_r + 1$ elements whose positions are

$$\{md_t, m = -M, -M+1, \ldots, M, M = N_tN_r\}. \tag{18}$$

An illustration for comparing the conventional and proposed two-level nested-arrays at $N_t = N_r = 3$ is shown in Fig. 3. While the optimal choices of N_t and N_r and the DOFs of the conventional and proposed two-level nested-arrays in the general case are depicted in Table 1. According to Table 1, in order to maximize the DOFs in the modified two-level nested-array, we should choose

$$N_t = N_r, \quad N \text{ is even} \tag{19a}$$

$$N_t = N_r \pm 1, \quad N \text{ is odd}. \tag{19b}$$

The first-level is used for both transmission and reception, while the second-level is used only for reception. In this case, the transmit-receive array can be further divided into two parts: One is the first-level (transmit) to the first-level (receive), which is just a traditional ULA without grating lobes in the transmit-receive beampattern. The second part is the first-level (transmit) to the second-level (receive), which is just the array configuration discussed in (3)-(8). In this

TABLE 1. **Comparison between conventional and proposed two-level nested-arrays for a given element number N.**

N	Optimal N_t and N_r	Conventional nested-array DOFs	Modified nested-array DOFs
even	$N_t = N_r = \frac{1}{2}N$	$\frac{N^2-2}{2} + N$	$\frac{N^2}{2} + 1$
odd	$N_t = \frac{N-1}{2}$, $N_r = \frac{N+1}{2}$	$\frac{N^2-1}{2} + N$	$\frac{N^2-1}{2} + 1$

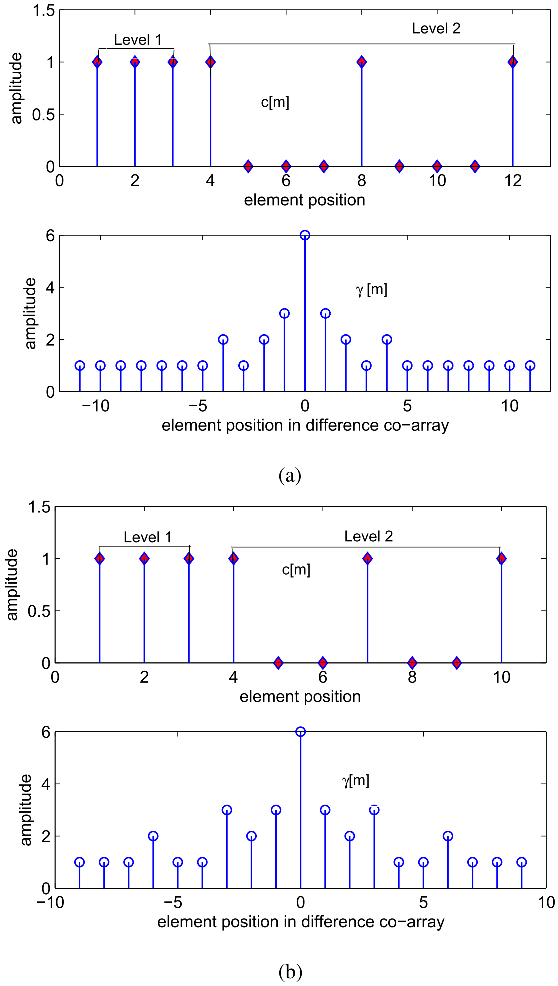

FIGURE 3. **Comparison between conventional and proposed two-level nested-arrays. In the former, both arrays are receivers while in the latter, the first level corresponds to both transmitter and receiver while the second level acts as receiver. (a) Conventional two-level nested-array. (b) Proposed two-level nested-array.**

paper, we consider mainly the second part. In order to suppress the grating lobes, according to (9) the modified two-level nested-array elements should be deployed as

$$d_r = N_t d_t. \tag{20}$$

Correspondingly, the optimization problem of (13) is now:

$$\begin{aligned} &\min \{N_t + N_r\} \\ &\text{s.t. } \mathbf{c}_v = \mathbf{A}_t \mathbf{c}_t = \mathbf{A}_r \mathbf{c}_r \\ &\quad d_r = N_t d_t \\ &\quad N_t = N_r \text{ or } N_t = N_r \pm 1. \end{aligned} \tag{21}$$

The last issue we need to address is the fulfillment of the transmit-receive pattern requirement of $p_v(x)$. For the special case when $p_v(x)$ can be expressed as a unity-coefficient polynomial, the polynomial factorization method [27] can be applied. Take $p_v(x) = \sum_{i=0}^{11} x^i$ as an example. The $11 + 1 = 12$ can be decomposed into three prime integers 3, 2 and 2, i.e., $12 = 3 \times 2 \times 2$. Then $p_v(x)$ can be factorized as

$$p_v(x) = \left(1 + x + x^2\right)\left(1 + x^3\right)\left(1 + x^6\right). \tag{22}$$

An optimal combination that satisfies (22) is

$$p_t(x) = 1 + x + x^2 \tag{23a}$$
$$p_r(x) = 1 + x^3 + x^6 + x^9. \tag{23b}$$

This requires 7 elements, namely, 3 and 4 antennas in the first- and second-level arrays, respectively. However, this method can be used only for the $p_v(x)$ which is a unity-coefficient polynomial. Moreover, for a large-scale array with thousands of elements, it is difficult to get the optimum decomposition for the high-order polynomial because there is no closed-form expression for the structure.

For an arbitrary $p_v(x)$ and a given number of available physical elements, this paper uses the LS method which is presented as follows. Suppose there are a total of N available physical elements and the desired effective element position vector $\mathbf{c}_v^{\text{new}}$ is known. Note that, to avoid confusing with the variables defined in Section II, a superscript "new" is added in this section. Without loss of generality, we assume that N is an even integer. In this case, we first design the second-level array with $N_r = N/2$ elements where $N_t \cdot \frac{\lambda}{2} = \frac{N}{2} \cdot \frac{\lambda}{2}$. The receive vector $\mathbf{c}_r^{\text{new}} \in \mathbb{C}^{[(N_t-1)N_r+1]\times 1}$ can then be modeled as

$$\mathbf{c}_r^{\text{new}} = \left[c_r[0]\ \overbrace{0\ldots0}^{N_t-1}\ c_r[N_t]\ \ldots\ \overbrace{0\ldots0}^{N_t-1}\ c_r[(N_t-1)N_r] \right]^T \tag{24}$$

where $c_r[\cdot]$ are constants which are not necessarily one and can even be complex-valued. The $N_t N_r \times N_r$ matrix $\mathbf{A}_t$ defined in (11a) can be expressed as (25).

$$\mathbf{A}_t = \begin{bmatrix} \mathbf{c}_r^{\text{new}} & & & \\ & \mathbf{c}_r^{\text{new}} & & \\ & & \ddots & \\ & & & \mathbf{c}_r^{\text{new}} \end{bmatrix} \tag{25}$$

Since he matrix $\mathbf{A}_t$ is a full-rank matrix. The $N_r \times 1$ transmit vector $\mathbf{c}_t^{\text{new}} = \left[c_t[0]\ c_t[1]\ \ldots\ c_t[N_t-1]\right]^T$ can then be determined by LS:

$$\begin{aligned} &\min \| \mathbf{c}_v^{\text{new}} - \mathbf{A}_t \mathbf{c}_t^{\text{new}} \|^2, \quad \min \| \mathbf{c}_V^{\text{new}} - \mathbf{A}_r \mathbf{c}_r^{\text{new}} \|^2 \\ &\text{s.t. } c_t[i] \neq 0, \quad i = 0, 1, \ldots, N_t - 1 \\ &c_r[i \cdot N_r] \neq 0, \quad i = 0, 1, \ldots, N_t - 1 \end{aligned} \tag{26}$$

where the cost functions $c_t[i] \neq 0, \quad i = 0, 1, \ldots, N_t - 1$ and $c_r[i \cdot N_r] \neq 0, \quad i = 0, 1, \ldots, N_t - 1$ are imposed to achieve the relation (21), namely, $d_r = N_t d_t$, to formulate the modified nested-array.

By solving (26), all the array parameters will be determined such that the requirements of suppressing grating lobes and maximizing DOFs are met simultaneously. The proofs of the solution uniqueness and convergence are provided in the *Appendix*. The complexity order of (26) is $\mathcal{O}\left(N_t\,(R_e + T_e - 1)\,T_e + N_t T_e^2\right)$.

To summarize, the design steps are:

(i) Based on the design specifications such as mainlobe width and sidelobe levels, determine the effective transmit-receive aperture function $p_v(x)$, and its order is denoted as M.
(ii) Determine the required transmit and receive element numbers N_t and N_r such that $N_t N_r \geq M$ and $N_t = N_r$ or $N_t = N_r \pm 1$.
(iii) The $p_t(x)$ and $p_r(x)$ are obtained by solving (26). Check the transmit and receive element positions to make sure that $d_r = N_t d_t$.
(iv) Check the grating lobes and compute the DOFs. If the design specifications are not met, go back to Step (iii) to recalculate $p_t(x)$ and $p_r(x)$ by tuning the vector $\mathbf{c}_r^{\text{new}}$, namely, $\mathbf{A}_t^{\text{new}}$.

IV. MODIFIED NESTED-ARRAY FOR BEAMFORMING AND DIRECTION FINDING

The performance of the modified nested-array in adaptive beamforming and direction finding can be similarly analyzed as [29]. Let $\mathbf{a}(\theta)$ be the $N \times 1$ receive steering vector corresponding to the direction θ whose i-th element is $e^{j(2\pi/\lambda)d_i \sin\theta}$ with d_i denoting the position of the i-element. Here, the first element is taken as the reference. Suppose D narrowband sources impinge on this array from distinct directions θ_i ($i = 1, 2, \ldots, D$) with powers σ_i^2 ($i = 1, 2, \ldots, D$), respectively. The received signal is expressed as

$$\mathbf{x}(t) = \mathbf{A}\mathbf{s}(t) + \mathbf{n}(t) \tag{27}$$

where $\mathbf{A} = \left[\mathbf{a}(\theta_1)\ \mathbf{a}(\theta_2)\ \ldots\ \mathbf{a}(\theta_D)\right]$ is the array manifold matrix, $\mathbf{s} = \left[s_1(t)\ s_2(t)\ \ldots\ s_D(t)\right]^T$ is the source signal vector, and $\mathbf{n}(t)$ is the noise vector which is assumed to be temporally and spatially white and uncorrelated with the sources.

The covariance matrix is

$$\mathbf{R}_{xx} = E\left\{\mathbf{x}(t)\mathbf{x}^H(t)\right\} = \mathbf{A}\mathbf{R}_{ss}\mathbf{A}^H + \sigma_n^2\mathbf{I}_N \tag{28}$$

where E represents the expectation operator, ^{H} is the conjugate transpose, $\mathbf{R}_{ss} = E\left\{\mathbf{s}(t)\mathbf{s}^H(t)\right\}$ is the source auto-correlation matrix, σ_n^2 is the noise variance and $\mathbf{I}_N$ is the $N \times N$ identity matrix. When the sources are temporally uncorrelated, $\mathbf{R}_{xx}$ can be vectorized as [41]

$$\mathbf{z} = \text{vec}\left(\mathbf{R}_{xx}\right) = \sum_{i=1}^{D}\left[\mathbf{a}^*(\theta_i) \otimes \mathbf{a}(\theta_i)\right]\sigma_i^2 + \sigma_n^2\text{vec}(\mathbf{I}_N) \tag{29}$$

where vec(·) is the vectorization operator, * is the conjugate operator and $\otimes$ is the Kronecker product. It is noticed from (29) that the grating lobes are suppressed due to the fact that the difference co-array processing scheme will produce a non-sparse uniform linear array.

Next, analogous to [29], forward-backward spatial smoothing and multiple signal classification (MUSIC) techniques can then be adopted to estimate the direction-of-arrival (DOA) of targets by exploiting he $N^2 \times 1$ vector $\mathbf{z}$.

V. SIMULATION RESULTS

In the following simulations, we assume that the array operates at a carrier frequency 10 GHz. The additive noise is modeled as a complex Gaussian zero-mean spatially and temporally white random sequence that has identical variance in the array.

Example 1: Unity-Coefficient Polynomial Array Beampattern Design

In the first example, a sparse array is designed, where the corresponding transmit-receive aperture function can be expressed as a unity-coefficient polynomial, $p_v(x) = \sum_{i=0}^{24} x^i$. According to the design steps presented in Section III, to implement the polynomial order $M = 24$, the number of transmit and receive elements should be chosen as $N_t = 5$ and $N_r = 5$, respectively. The receive array elements are arranged as (24) and construct the full-rank matrix $\mathbf{A}_r$ of (25). The $c_t[i]$ and $c_r[iN_r]$ with $i = 0, 1, \ldots, N_1 - 1$, can then be obtained through (26).

This special unity-coefficient array beampattern can also be designed with the polynomial factorization method [17], [27]. In this case, the $24 + 1 = 25$ is factorized into two prime integers 5 and 5, that is, $25 = 5 \times 5$. Then, $p_v(x)$ can then be factorized as $p_v(x) = \left(1 + x + x^2 + x^3 + x^4\right)\left(1 + x^5 + x^{10} + x^{15} + x^{20}\right)$. According to (21), the transmit and receive elements can be arranged as $p_t(x) = \left(1 + x + x^2 + x^3 + x^4\right)$ and $p_r(x) = \left(1 + x^5 + x^{10} + x^{15} + x^{20}\right)$. That is to say, it requires 5 transmit elements and 5 receive elements. They are placed at the positions $\{0, d, 2\,d, 3\,d, 4\,d\}$ and $\{0, 4d, 9\,d, 14\,d, 19\,d\}$ with $d = \lambda/2$, respectively. Fig. 4 compares the LS solution with the polynomial factorization method in designing the array. We cannot see the difference between the two results shown in Fig. 4(b)-(c) and (d)-(e). Therefore, we can conclude that for unity-coefficient array beampattern, similar results can be obtained for the LS and polynomial factorization methods, but the former is advantageous in designing large-scale arrays.

Suppose the array direction angle is $\theta = 0°$. Fig. 5(a)-(c) show the comparative transmit, receive and effective transmit-receive array patterns, respectively. It is noticed that the transmit array nulls and receive array grating peaks have the same positions. The receive array grating lobes are effectively suppressed due to the null-grating-lobe compensation scheme and thus the final transmit-receive array pattern has no grating lobes.

Example 2: Arbitrary Array Beampattern Design

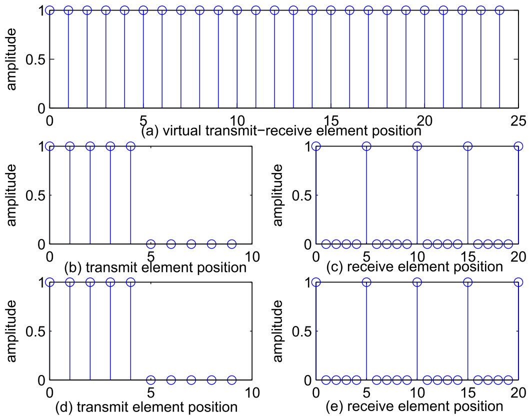

FIGURE 4. Illustration of transmit and receive array arrangement: (a) virtual transmit-receive aperture function, (b)-(c) and (d)-(e) are designed with the LS method and conventional polynomial factorization method, respectively.

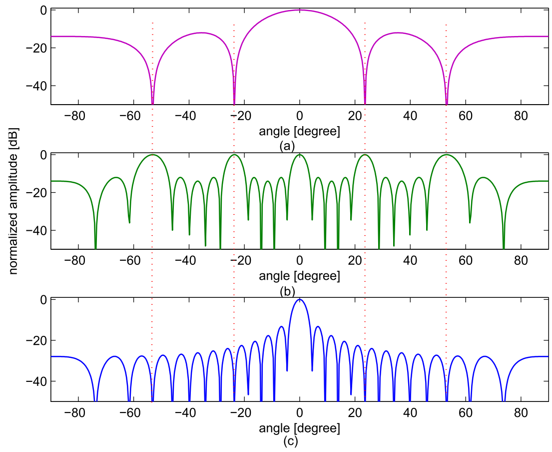

FIGURE 5. Comparative transmit, receive and effective array patterns: (a) transmit array pattern, (b) receive array pattern, and (c) effective transmit-receive array pattern.

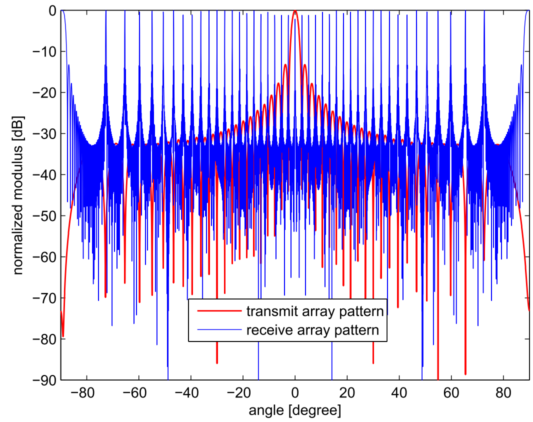

FIGURE 6. Comparative transmit and receive array patterns.

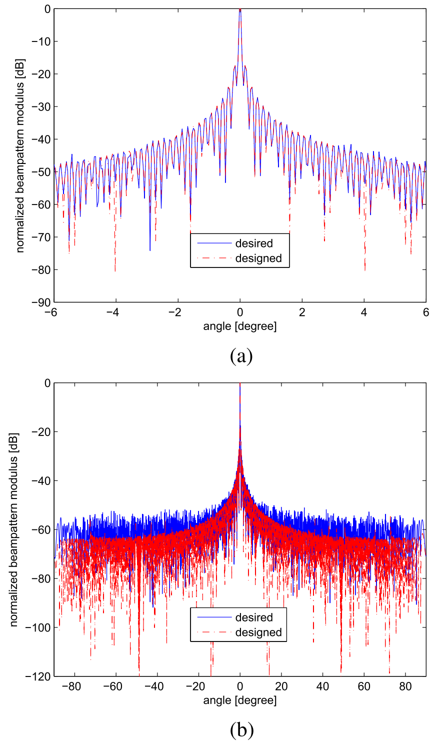

FIGURE 7. Desired and designed transmit-receive array patterns. (a) Mainlobe view. (b) Overall view.

In the second example, we consider a more general array design using the LS method. Suppose the desired effective transmit-receive array pattern is $p_v(x) = \sum_{i=0}^{1935} c_v[i]x^i$, where $c_v[i]$ are real or complex coefficients. For such a high-order polynomial, it is difficult to find the suitable $p_t(x)$ and $p_r(x)$ with the polynomial factorization method [17], [27], because there will be many different decomposition combinations. Without loss of generality, we assign $c_v[i] = 1+2j+0.25\,n[i]$, where $n[i]$ is a uniformly distributed random variable and the j-related term denotes the complex component. According to the LS method, both the transmit and receive arrays use 44 elements, i.e, $N_t = N_r = 44$. First, we arrange the receive elements as (24) and construct the full-rank matrix $\mathbf{A}_t^{\text{new}}$ of (25). Next, the $c_t[i]$ and $c_r[iN_r]$ with $i = 0, 1, \ldots, N_1 - 1$, can then be obtained through (26). Fig. 6 shows the comparative transmit and receive array patterns. The transmit array nulls and receive array grating peaks have the same positions and thus the grating lobes are suppressed in the receiver. Fig. 7 compares the designed and desired effective transmit-receive array patterns. It is seen that they are perfectly matched in the array mainlobe (see Fig. 7(a)). Moreover, the designed array pattern has lower sidelobes (see Fig. 7(b)). This is of great importance in detecting small targets in phased-array radar applications.

Example 3: Rectangular Beampattern Synthesis

In this example, an arbitrary rectangular beampattern is designed. Without loss of generality, suppose the rectangular beampattern can be expressed as a gate function: $p_v(\theta) = 1000$ when $|\theta| \leq \pi/18$; otherwise, $p_v(\theta) = 1$. This beampattern cannot be synthesized with the polynomial factorization method [17], [27], but it can be easily implemented with the LS method. First, we approximate the expected

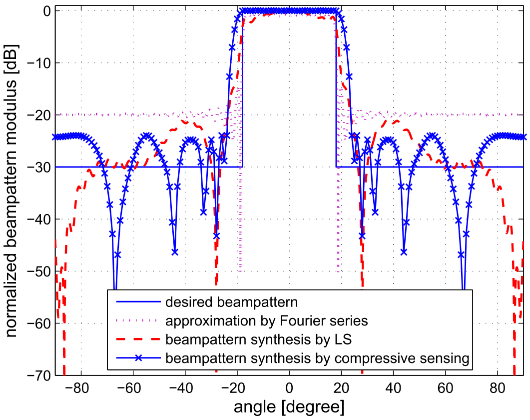

FIGURE 8. Rectangular beampattern synthesis comparisons.

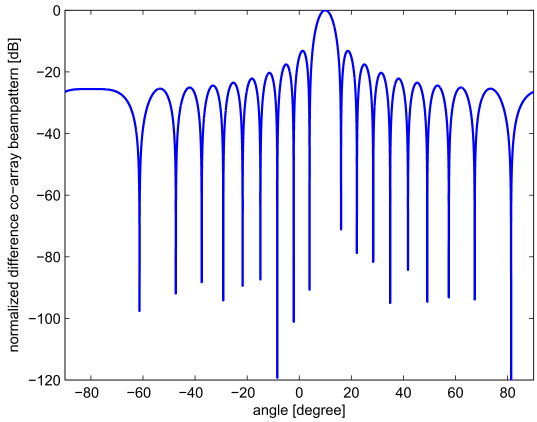

FIGURE 9. Difference co-array beampattern.

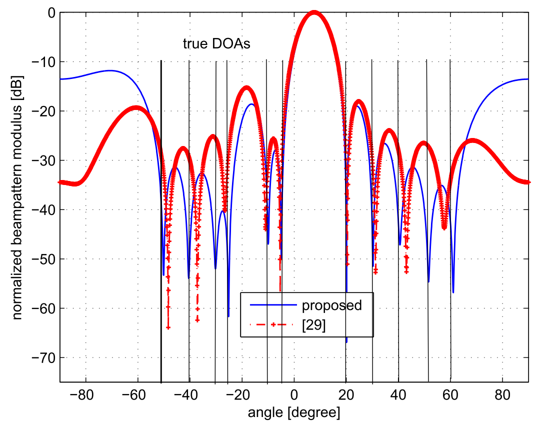

FIGURE 10. Comparative MVDR-like beamforming results.

beampattern function as Fourier series, namely $p_v(\theta) = \frac{a_0}{2} + \sum_{m=1}^{M-1} a_m \cos(n\theta)$, where a_m, $m = 0, 1, \ldots, M-1$, are the Fourier series coefficients. The approximation errors can be reduced by choosing a sufficiently large value of M which will increase the required number of array elements to synthesize the beampattern. As a compromise, $M = 100$ is chosen in the simulation example. According to the presented design steps, the numbers of transmit and receive elements are determined as $N_t = N_r = 10$. Then, the transmit and receive array parameters are obtained using (26). Figure 8 compares the beampattern synthesis with conventional Fourier series and compressive sensing methods. It is observed that satisfactory beampattern synthesis performance has been obtained by the LS method. Certainly the beampattern flatness in the mainlobe can be further improved by choosing a large M, but it means that more array elements are required.

Example 4: Difference Co-Array Processing-Based Beamforming and DOA Estimation

Finally, the difference co-array processing-based beamforming and DOA estimation performance are analyzed. Suppose there are 6 physical elements, which are arranged as the modified two-level nested-array and the array direction angle is 10°. As all the elements receive the signals, when the difference co-array processing algorithm is employed, we can calculate the difference co-array beampattern. When the non-adaptive beamformer is used, the corresponding difference co-array beampattern is $B_{\text{power}}(\theta) = \|\mathbf{a}^*(\theta) \otimes \mathbf{a}(\theta)\|^2$, as shown in Fig. 9. Obviously, it has 18 nulls and thus gives 19 DOFs. This validates from Table 1 that for N elements, we can obtain $\frac{N^2}{2} + 1 = 19$ DOFs.

Further suppose there are 11 interferences at directions $\{-50°, -40°, -30°, -25°, -10°, -5°, 20°, 30°, 40°, 50°, 60°\}$. The spatially smoothed covariance matrix $\mathbf{R}_{zz}$ is computed with 500 snapshots. Suppose both the signal-to-noise ratio and interference-to-noise ratio (SNR) are 10 dB, Fig. 10 compares the minimum variance distortionless response (MVDR)-like beamforming results of our method with [29]. Although the proposed method suppresses grating lobes at a cost of less DOFs than [29] (see Table 1), it achieves more DOFs by employing the forward-backward spatial smoothing method. For instance, the interferences at $\{-30°, 50°\}$ are not effectively nulled in [29]. In contrast, in the proposed method all the interferences are automatically nulled in their directions even without explicitly knowing the interference DOAs. Suppose we want to estimate the DOAs of the 11 interference sources, namely, at directions $\{-50°, -40°, -30°, -25°, -10°, -5°, 20°, 30°, 40°, 50°, 60°\}$. Fig. 11 shows one realization of the DOA spectrum of the MUSIC estimator with forward-backward spatial smoothing for the 11 interference sources. It is seen that, the peaks of the spectrum are in good agreement with their true DOAs.

Using the same simulation settings, a Monte Carlo simulation is carried out to evaluate the root mean square error (RMSE) performance. The number of Monte Carlo trials is 500. Fig. 12 compares the RMSE performance of angle estimation for four sources located at $\{-40°, -10°, 20°, 30°\}$. Here, the RMSE is defined as $\sqrt{\left[\sum_{i=1}^{4}(\theta_i - \hat{\theta}_i)^2\right]/4}$, where θ_i and $\hat{\theta}_i$ denote the true and estimated angles, respectively. It is seen that the proposed method gives a little bit better RMSE performance due to the forward-backward spatial smoothing.

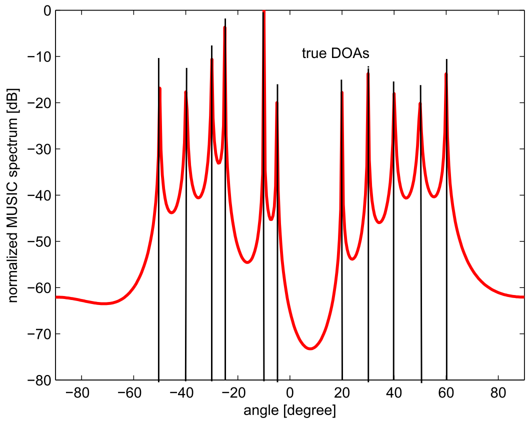

FIGURE 11. DOA spectrum of the MUSIC estimator with forward-backward spatial smoothing for the 11 interference sources.

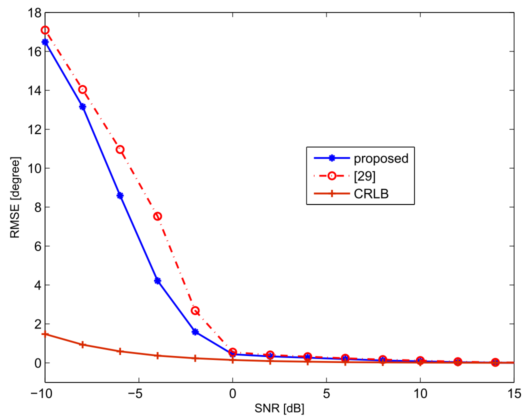

FIGURE 12. Comparative RMSE performance of angle estimation versus SNR.

VI. CONCLUSION

This paper proposed an LS algorithm to design an arbitrary array beampattern synthesis and a modified two-level nested-array which suppresses grating lobes and simultaneously provides increased DOFs. When compared to the basic nested-array, the modified nested-array suppresses the grating lobes at a cost of less DOFs. Note that, since the grating lobes suppression scheme is independent on the actual steering direction, the grating lobes can be suppressed when it steers away from broadside. Moreover, a forward-backward spatial smoothing algorithm is used to develop the MVDR beamformer and MUSIC estimator. The proposed method allows the design of desired transmit-receive beampattern with a reduced number of non-uniformly spaced active elements and without grating lobes. It excels the conventional polynomial factorization method in designing a large and/or arbitrary array. The proposed nested-array is motivated by two facts, namely, grating lobes can be suppressed by optimum arrangement of array elements, and more DOFs can be obtained than a standard ULA with the same number of elements by the difference co-array processing algorithm. In the proposed design, the real antenna array spacing is integer multiple of half of the wavelength. These spacings are implementable in practical array systems. Note that the proposed method is able to provide closed-form expressions for the sensor locations and the exact DOFs as a function of the total number of sensors, which may be a difficulty for conventional methods. This paper only considers linear one-dimensional arrays, two-dimensional arrays will be further investigated in future work. Jointly utilizing phased-MIMO and FDA is also an interesting future work. Another future work is to analyze the coupling effects on the array performance.

APPENDIX
DISCUSSIONS OF SOLUTION UNIQUENESS AND CONVERGENCE OF (26)

The (26) is a polynomial blind decomposition problem that can be handled by the LS and iterative algorithm [42]. For notation simplicity, the superscript "New" is ignored in this appendix. The LS algorithm can be implemented as follows:

(1) According to the desired transmit-receive array beampattern, determine first the values of N_t and N_r.

(2) According (24) and (25), determine the structures of $\mathbf{c}_r$, $\mathbf{A}_t$ and $\mathbf{c}_t$.

(3) Using the initially guessed $\mathbf{c}_r^{(k)}$ to formulate $\mathbf{A}_t^{(k)}$:

$$\mathbf{A}_t^{(k)} = \begin{bmatrix} \mathbf{c}_r^{(k)} & & & \\ & \mathbf{c}_r^{(k)} & & \\ & & \ddots & \\ & & & \mathbf{c}_r^{(k)} \end{bmatrix}. \tag{30}$$

(4) We then have

$$\min \left\| \mathbf{c}_v - \mathbf{A}_t^{(k)} \mathbf{c}_t^{(k)} \right\|^2, \quad k = 0, 1, \ldots \tag{31}$$

Consider again $\mathbf{A}_t$ expressed in (25). Since $c_r[0] \neq 0$ is assumed, it is easily proved that the $\mathbf{A}_t^{(k)}$ is a full-rank matrix. Using the well-known LS algorithm, the above (31) has the unique solution:

$$\mathbf{c}_t^{(k)} = \left[\left(\mathbf{A}_t^{(k)} \right)^T \mathbf{A}_t^{(k)} \right]^{-1} \left(\mathbf{A}_t^{(k)} \right)^T \mathbf{c}_v. \tag{32}$$

(5) Using $\mathbf{c}_t^{(k)}$ to construct $\mathbf{A}_r^{(k)}$ similar to (25) and (11b) as follows

$$\mathbf{A}_r^{(k)} = \begin{bmatrix} \mathbf{c}_t^{(k)} & & & \\ & \mathbf{c}_t^{(k)} & & \\ & & \ddots & \\ & & & \mathbf{c}_t^{(k)} \end{bmatrix}. \tag{33}$$

(6) Formulate the following problem

$$\min \left\| \mathbf{c}_v - \mathbf{A}_r^{(k)} \mathbf{c}_r^{(k+1)} \right\|^2, \quad k = 0, 1, \ldots \tag{34}$$

Similarly, since $\mathbf{A}_r^{(k)}$ is a full-rank matrix, we can get a unique solution:

$$\mathbf{c}_r^{(k+1)} = \left[\left(\mathbf{A}_r^{(k)} \right)^T \mathbf{A}_r^{(k)} \right]^{-1} \left(\mathbf{A}_r^{(k)} \right)^T \mathbf{c}_v. \tag{35}$$

(7) Let $k = k + 1$, rerun from Step (3) again to make the algorithm converge to a given threshold. At each step, the LS algorithm produces a unique solution. That is, we have the estimation sequences:

$$\mathbf{c}_t^{(0)}, \quad \mathbf{c}_t^{(1)}, \ \mathbf{c}_t^{(2)}, \ \ldots \tag{36a}$$

$$\mathbf{c}_r^{(0)}, \ \mathbf{c}_r^{(1)}, \ \mathbf{c}_r^{(2)}, \ldots. \tag{36b}$$

(8) Considering also (12) and that all $\mathbf{A}_t^{(k)}$ and $\mathbf{A}_r^{(k)}$ are full matrices, we then have

$$\left\|\mathbf{c}_v - \mathbf{A}_t^{(0)}\mathbf{c}_t^{(0)}\right\|^2 = \left\|\mathbf{c}_v - \mathbf{A}_r^{(0)}\mathbf{c}_r^{(0)}\right\|^2 \geq \left\|\mathbf{c}_v - \mathbf{A}_r^{(1)}\mathbf{c}_r^{(1)}\right\|^2 \geq \ldots \geq 0. \tag{37}$$

In doing so, the transmit and receive array weighting coefficients can be designed with the solutions when $k \to \infty$.

REFERENCES

[1] J. Li and P. Stoica, "The phased array is the maximum SNR active array," *IEEE Signal Process. Mag.*, vol. 27, no. 2, pp. 143–144, Feb. 2010.

[2] A. Manikas, Y. I. Kamil, and M. Willerton, "Source localization using sparse large aperture arrays," *IEEE Trans. Signal Process.*, vol. 60, no. 12, pp. 6617–6629, Dec. 2012.

[3] M. Rubsamen and A. B. Gershman, "Sparse array design for azimuth direction-of-arrival estimation," *IEEE Trans. Signal Process.*, vol. 59, no. 12, pp. 5957–5969, Dec. 2011.

[4] N. Hu, Z. Ye, X. Xu, and M. Bao, "DOA estimation for sparse array via sparse signal reconstruction," *IEEE Trans. Aerosp. Electron. Syst.*, vol. 49, no. 2, pp. 760–773, Apr. 2013.

[5] T. Li and A. Nehorai, "Maximum likelihood direction finding in spatially colored noise fields using sparse sensor arrays," *IEEE Trans. Signal Process.*, vol. 59, no. 3, pp. 1048–1062, Mar. 2011.

[6] L. Lei, J. P. Lie, A. B. Gershman, and C. M. S. See, "Robust adaptive beamforming in partly calibrated sparse sensor arrays," *IEEE Trans. Signal Process.*, vol. 58, no. 3, pp. 1661–1667, Mar. 2010.

[7] M. Kleinsteuber and A. K. Seghouane, "On the deterministic CRB for DOA estimation in unknown noise fields using sparse sensor arrays," *IEEE Trans. Signal Process.*, vol. 56, no. 2, pp. 860–864, Feb. 2008.

[8] S. A. Vorobyov, A. B. Gershman, and K. M. Wong, "Maximum likelihood direction-of-arrival estimation in unknown noise fields using sparse sensor arrays," *IEEE Trans. Signal Process.*, vol. 53, no. 1, pp. 34–43, Jan. 2005.

[9] L. Cen, L. Y. Zhu, W. Ser, and W. Cen, "Linear aperiodic array synthesis using an improved genetic algorithm," *IEEE Trans. Antennas Propag.*, vol. 60, no. 2, pp. 895–902, Feb. 2012.

[10] G. Oliveri and A. Massa, "Genetic algorithm (GA)-enhanced almost difference set (ADS)-based approach for array thinning," *IET Microw., Antennas Propag.*, vol. 5, no. 3, pp. 305–315, Feb. 2011.

[11] K. S. Tang, K. F. Man, S. Kwong, and Q. He, "Genetic algorithms and their applications," *IEEE Signal Process. Mag.*, vol. 13, no. 6, pp. 22–37, Nov. 1996.

[12] L. Carin, D. Liu, and B. Guo, "Coherence, compressive sensing, and random sensor arrays," *IEEE Antennas Propag. Mag.*, vol. 53, no. 4, pp. 28–39, Aug. 2011.

[13] D. G. Leeper, "Isophoric arrays-massively thinned phased arrays with well-controlled sidelobes," *IEEE Trans. Antennas Propag.*, vol. 47, no. 12, pp. 1825–1835, Dec. 1999.

[14] G. Oliveri, F. Caramanica, M. D. Migliore, and A. Massa, "Synthesis of nonuniform MIMO arrays through combinatorial sets," *IEEE Antennas Wireless Propag. Lett.*, vol. 11, no. 11, pp. 728–731, 2012.

[15] R. M. Leahy and B. D. Jeffs, "On the design of maximally sparse beamforming arrays," *IEEE Trans. Antennas Propag.*, vol. 39, no. 8, pp. 1178–1187, Aug. 1991.

[16] M. Donelli, A. Martini, and A. Massa, "A hybrid approach based on PSO and Hadamard difference sets for the synthesis of square thinned arrays," *IEEE Trans. Antennas Propag.*, vol. 57, no. 8, pp. 2491–2495, Aug. 2009.

[17] G. Lockwood, P. Li, M. O'Donnell, and F. Foster, "Optimizing the radiation pattern of sparse periodic linear arrays," *IEEE Trans. Ultrason., Ferroelect., Freq. Control*, vol. 43, no. 1, pp. 7–14, Jan. 1996.

[18] F. Viani, G. Oliveri, and A. Massa, "Compressive sensing pattern matching techniques for synthesizing planar sparse arrays," *IEEE Trans. Antennas Propag.*, vol. 61, no. 9, pp. 4577–4587, Sep. 2013.

[19] G. Oliveri and A. Massa, "Bayesian compressive sampling for pattern synthesis with maximally sparse non-uniform linear arrays," *IEEE Trans. Antennas Propag.*, vol. 59, no. 2, pp. 467–481, Feb. 2011.

[20] K. Teramoto and H. Kamiirisa, "Reduction of the grating lobes in sparse array holographic sonar by projection onto convex sets," in *Proc. Int. Conf. Acoust., Speech, Signal Process.*, Detroit, MI, USA, May 1995, pp. 3639–3642.

[21] T. J. Brockett and Y. R. Samii, "Subarray design diagnostics for the suppression of undesirable grating lobes," *IEEE Trans. Antennas Propag.*, vol. 60, no. 3, pp. 1373–1380, Mar. 2012.

[22] P. V. Brennan, A. Narayanan, and R. Benjamin, "Grating lobe control in randomised, sparsely populated MIMO radar arrays," *IET Radar, Sonar Navigat.*, vol. 6, no. 7, pp. 587–594, Aug. 2012.

[23] H. Cox and H. Lai, "Simultaneous grating lobe and backlobe rejection with a linear array of vector sensors," in *Proc. 43rd Asilomar Conf. Signals, Syst. Comput.*, Pacific Grove, CA, USA, Nov. 2009, pp. 1320–1323.

[24] R. L. Haupt, "Unit circle representation of aperiodic arrays," *IEEE Trans. Antennas Propag.*, vol. 43, no. 10, pp. 1152–1155, Oct. 1995.

[25] S. U. Pillai, Y. Bar-Ness, and F. Haber, "A new approach to array geometry for improved spatial spectrum estimation," *Proc. IEEE*, vol. 73, no. 10, pp. 1522–1524, Oct. 1985.

[26] D. A. Linebarger, I. H. Sudborough, and I. G. Tollis, "Design and analysis of distributed radar sensor networks," *IEEE Trans. Parallel Distrib. Syst.*, vol. 22, no. 11, pp. 1926–1933, Nov. 2011.

[27] S. K. Mitra, K. Mondal, M. K. Tchobanou, and G. Jovanovic, "General polynomial factorization-based design of sparse periodic linear arrays," *IEEE Trans. Ultrason., Ferroelect., Freq. Control*, vol. 57, no. 9, pp. 1952–1966, Sep. 2010.

[28] R. T. Hoctor and S. A. Kassam, "The unifying role of the coarray in aperture synthesis for coherent and incoherent imaging," *Proc. IEEE*, vol. 78, no. 4, pp. 735–752, Apr. 1990.

[29] P. Pal and P. P. Vaidyanathan, "Nested arrays: A novel approach to array processing with enhanced degrees of freedom," *IEEE Trans. Signal Process.*, vol. 58, no. 8, pp. 4167–4181, Aug. 2010.

[30] P. Pal and P. P. Vaidyanathan, "A novel array structure for directions-of-arrival estimation with increased degrees of freedom," in *Proc. IEEE Int. Conf. Acoust., Speech Signal Process.*, Dallas, TX, USA, Mar. 2010, pp. 2606–2609.

[31] P. Pal and P. P. Vaidyanathan, "Beamforming using passive nested arrays of sensors," in *Proc. IEEE Int. Symp. Circuits Syst.*, Paris, France, Jun. 2010, pp. 2840–2843.

[32] P. Pal and P. P. Vaidyanathan, "Nested arrays in two dimensions, part I: Geometrical considerations," *IEEE Trans. Signal Process.*, vol. 60, no. 9, pp. 4694–4705, Sep. 2012.

[33] W.-Q. Wang and C. L. Zhu, "Nested array receiver with time-delayers for joint target range and angle estimation," *IET Radar, Sonar Navigat.*, vol. 10, no. 8, pp. 1384–1393, Oct. 2016.

[34] H. Commin and A. Manikas, "Virtual SIMO radar modelling in arrayed MIMO radar," in *Proc. Sensor Signal Process. Defence (SSPD)*, Sep. 2012, pp. 1–6.

[35] T. Baran, D. Wei, and A. V. Oppenheim, "Linear programming algorithms for sparse filter design," *IEEE Trans. Signal Process.*, vol. 58, no. 3, pp. 1605–1617, Mar. 2010.

[36] K. Adhikari, J. R. Buck, and K. E. Wage, "Extending coprime sensor arrays to achieve the peak side lobe height of a full uniform linear array," *EURASIP J. Adv. Signal Process.*, vol. 1, no. 148, pp. 1–17, 2014.

[37] C.-L. Liu and P. P. Vaidyanathan, "Comprime DFT filter bank design: Theoretical bounds and guarantees," in *Proc. IEEE Int. Conf. Acoust., Speech Signal Process.*, Brisbane, QLD, Australia, Apr. 2015, pp. 3861–3865.

[38] T. G. Kolda and B. W. Bader, "Tensor decompositions and applications," *SIAM Rev.*, vol. 51, no. 3, pp. 455–500, 2009.

[39] P. F. Sammartino, D. Tarchi, and C. J. Baker, "MIMO radar topology: A systematic approach to the placement of the antennas," in *Proc. Int. Conf. Electromagn. Adv. Appl.*, Turin, Italy, Sep. 2011, pp. 114–117.

[40] W.-Q. Wang, *Multi-Antenna Synthetic Aperture Radar*. New York, NY, USA: CRC Press, May 2013.

[41] W.-K. Ma, T.-H. Hsieh, and C.-Y. Chi, "DOA estimation of quasi-stationary signals with less sensors than sources and unknown spatial noise covariance: A Khatri–Rao subspace approach," *IEEE Trans. Signal Process.*, vol. 58, no. 4, pp. 2168–2179, Apr. 2010.
[42] M.-Y. Zou and R. Unbenauen, "Approximate factorization of multivariable polynomials," *Signal Process.*, vol. 14, no. 2, pp. 141–152, 1988.

ZHE WANG received the B.E. degree in electronic information and control engineering from the Beijing University of Technology, Beijing, China, in 2010. He is currently pursuing the Ph.D. degree in information and communication engineering with the University of Electronic Science and Technology of China. His research interests include radar signal processing and wireless communication.

WEN-QIN WANG (M'08–SM'16) received the B.S. degree in electrical engineering from Shandong University, Shandong, China, in 2002, and the M.E. and Ph.D. degrees in information and communication engineering from the University of Electronic Science and Technology of China (UESTC), Chengdu, China, in 2005 and 2010, respectively.

From 2005 to 2007, he was with the National Key Laboratory of Microwave Imaging Technology, Chinese Academy of Sciences, Beijing, China. Since 2007, he has been with the School of Information and Communication Engineering, UESTC, where he is currently a Professor and the Director of the Multi-Dimensional Information Sensing and Processing Research Centre. From 2011 to 2012, he was a Visiting Scholar with the Stevens Institute of Technology, Hoboken, NJ, USA. From 2012 to 2013, he was a Hong Kong Scholar with the City University of Hong Kong, Hong Kong. From 2014 to 2016, he was a Marie Curie Fellow with the Imperial College London, U.K. His research interests span the area of array signal processing and circuit systems for radar, communications, and microwave remote sensing.

ZHI ZHENG received the M.S. and Ph.D. degrees in electronic engineering and information and communication engineering from the University of Electronic Science and Technology of China (UESTC), Chengdu, China, in 2007 and 2011, respectively. Since 2011, he has been with the School of Communication and Information Engineering, UESTC. From 2014 to 2015, he was an Academic Visitor with the Department of Electrical and Electronic Engineering, Imperial College London. He is currently an Associate Professor with the School of Information and Communication Engineering, UESTC. His area of interests include wireless communications, signal processing for communications, array signal processing including robust adaptive beamforming, direction-of-arrival estimation and source localization, array processing for radar, communications applications, compressed sensing, and sparse signal processing.

HUAIZONG SHAO received the M.S. degree in electrical engineering from Sichuan University, Chengdu, China, in 1998, and the Ph.D. degree in information and communication engineering from the University of Electronic Science and Technology of China (UESTC), Chengdu, in 2003. Since 2003, he has been with the School of Information and Communication Engineering, UESTC, where he is currently a Professor. From 2014 to 2015, he was a Visiting Scholar with The University of Sheffield, Sheffield, U.K. His research interests include communication and radar signal processing.